1 Summaries of Experimental Activities

1.1 E12-07-108

Precision Measurement of the Proton Elastic Cross Section at High Q^2

J. Arrington, M. Christy, S. Gilad, B. Moffit, V. Sulkosky and B. Wojtsekhowski, spokespersons,
and
the Hall A collaboration.
contributed by V. Sulkosky and B. Wojtsekhowski, for the GMp collaboration.

The GMp experiment was proposed to measure the elastic electron-proton cross-section from 7 to 17 GeV^2 in Q^2 with an unprecedented precision of less than 2%. The experiment has two main goals. The first goal is a precise measurement of the proton elastic cross-section at the kinematics of the upgraded JLab 12 GeV facility for accurate normalization of other experiments. The second objective is to determine with improved precision the proton magnetic form-factor G_M^p at high Q^2. The JLab PAC recommended a beam time assignment of 24 days by asking the experimentalists not to pursue measurements at the two highest Q^2 points, which limits the highest planned Q^2 to 14 GeV^2.

The GMp and DVCS [1] experiments are scheduled to be the first two experiments to run after the 12 GeV upgrade in Hall A. The tentative plan is to concurrently run the two experiments to the greatest extent possible. The GMp collaboration is working in close contact with the DVCS collaboration, which will use the left high resolution spectrometer (HRS). Since the approval of the proposal, the collaboration has made a significant step in the instrumentation preparation which is briefly presented below.

1.1.1 Electron beam quality requirements

To achieve the goals outlined above, the GMp experiment requires the highest beam energy possible after the upgrade, $\sim$ 11 GeV into Hall A. The Q^2 range is achieved by using three standard beam energies (6.6 GeV, 8.8 GeV and 11 GeV) and two non-standard energies at 4.8 GeV and 5.8 GeV. These later two energies are necessary to study the ϵ dependence in order to constrain two photon exchange (TPE) corrections.

Of concern for the experiment is the accuracy of the beam energy. The current plan is to use the ARC energy method, which has provided a precision of $(3\text{–}4)\times10^{-4}$. The ARC energy system is in the process of being upgraded for the 12 GeV beam. After the upgrade, the system will be recalibrated using elastic scattering from hydrogen and tantalum targets with 2.2 GeV incident electrons. The beam stability and energy spread will be monitored by using the Optical Transition Radiation viewer, Synchrotron Light Interferometer and Tiefenback energy readback, the latter which is based on the beam positions from the beam position monitors (BPMs) located in the Hall A arc.

The incident beam angle can be determined by using the BPMs located near the target in Hall A with an uncertainty of 0.1 mrad. The beam charge is typically known to $\pm0.5\%$ with careful monitoring and calibration of the beam current monitors.

1.1.2 Detector configuration of the HRS spectrometers

The detector configuration, shown in Fig. 1, includes the vertical drift chambers (VDCs), the S0 and S2m counters, the Gas Cherenkov, the lead glass calorimeter, and one of the front FPP chambers.

The last is an existing detector used many times in the left HRS. It is the only non-standard item in an otherwise traditional electron arm configuration. By using this chamber, we plan to resolve a long-standing problem of HRS tracking analysis whose efficiency of track reconstruction is less than 95% in spite of a high chamber efficiency of 99.5%. For the VDCs, the amplifier/discriminator (A/D) cards are in the process of being replaced with those developed for the BigBite wire chambers [2]. These new cards use MAD chips [3], whose output stage works with LVDS signals, which produce significantly less feedback than ECL signals used in A/D cards by LeCroy Research Systems. This allows the VDCs to be operated at lower discriminator thresholds and high voltages. The status of these detectors is presented in Section **??**.

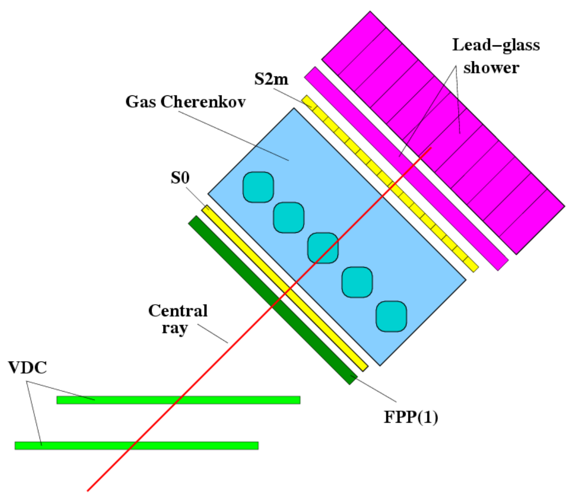

Figure 1: The planned detector configuration for the left and right HRSs for GMp with three wire chambers.

For the spectrometer optics calibration, a sieve-slit placed at the entrance to the spectrometers will be used to calibrate the solid angle acceptance, and carbon foils will be used along the beam line to calibrate the vertex position.

1.1.3 Configuration of the target

The standard Hall A cryogenic target ladder will be used with a liquid hydrogen target and carbon and aluminum solid targets for spectrometer optics calibrations and target background measurements, respectively. The thickness of the hydrogen target needs to be well defined. We plan to use 15 cm LH_2 "race-track" style cells that feature vertical flow of cryogenic fluid to reduce the effects of target density fluctuations. Earlier experiments used 20-cm long race-track cells.

Vertical-flow liquid hydrogen cell and performance

In 2002, tests had shown that the standard cigar-shaped cells displayed large density fluctuations with liquid hydrogen even with moderate beam currents at high fan speeds and large raster sizes. For this reason, the race-track cell [4] with vertical fluid flow was designed and built by the Cal State LA group in coordination with the JLab target group for the HAPPEx-II and HAPPEx-He experiments [5]. With the new race-track cells, the density fluctuations for an LH2 target were an order of magnitude smaller under similar raster sizes and fan speeds compared to the standard cells. The collaboration determined that with a 5 mm $\times$ 5 mm raster size that density fluctuations would contribute negligibly for a hydrogen target at 100 μA. However, during the 2005 run period, the fan speed had to be increased from the nominal 60 Hz to 91 Hz to minimize the density fluctuations. We plan to perform a detailed study of the density fluctuations from the race-track cell during commissioning of the experiment.

1.1.4 Swing arm wire target

Accurate knowledge of the scattering angle is very important in the GMp experiment. However, the mechanical stability of the Hall A spectrometers has a known problem, which could lead to a several mm displacement of the vertex. Regular checks of the spectrometer pointing by using the optics target mounted on the long ladder of the cryo-target provide an indication of stability but are insufficient for the level of accuracy needed in the GMp experiment. We have proposed a solution to this problem by using a tungsten wire target mounted on the scattering chamber via a short arm, see Fig. 2.

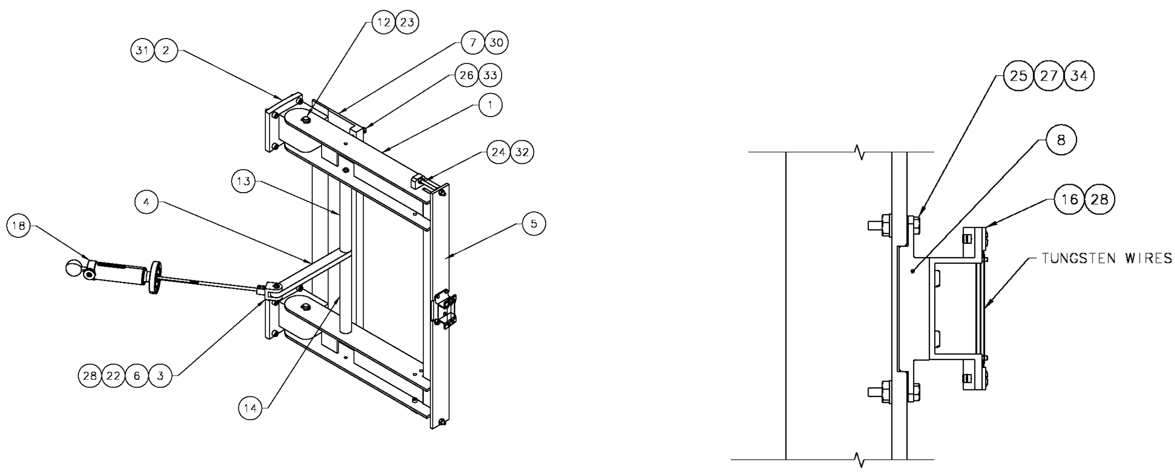

Figure 2: Shown is a schematic view of the swing arm target. The right-hand side figure illustrates the tungsten wires that will be placed in the beam.

1.1.5 Systematic Uncertainty and Expected Results

Achieving the total expected precision on the cross-section measurement requires serious work to minimize the systematic uncertainties on several parameters. Some of the most critical include the scattering angle, detector efficiencies, deadtime, spectrometer acceptance, target density and beam charge. A few of these items were discussed in the previous sections. The contributions to the total uncertainty expected on the differential cross section are summarized in Table 1.

In Figure 3, the published world data on the form factor G_M^p versus Q^2 is shown along with the range and uncertainties for the expected results of the planned experiment.

1.1.6 Summary

For the GMp experiment, we aim to measure the proton elastic cross section for $Q^2 = 7$–14 GeV^2 with a total precision of less than 2%. A few additional general purpose devices and improved analysis techniques will be used to aid our understanding of the systematic uncertainties. The

Source	$\Delta\sigma/\sigma$ (%)
Point to Point uncertainties	
Incident Energy	<0.3
Scattering Angle	0.1–0.3
Incident Beam Angle	0.1–0.2
Radiative Corrections*	0.3
Beam Charge	0.3
Target Density Fluctuations	0.2
Spectrometer Acceptance	0.4–0.8
Al Endcap Subtraction	0.1
Detector efficiencies and dead time	0.3
quadratic sum	0.8–1.1
Normalization uncertainties	
Beam Charge	0.4
Target Thicness/Density	0.5
Radiative Corrections*	0.4
Spectrometer Acceptance	0.6–1.0
Al Endcap Subtraction	0.1
Detector efficiencies and dead time	0.4
quadratic sum	1.0–1.3
Statistics	0.5–0.8
Total (Scale+Rand.+Stat.)	**1.2–1.7**

* Not including two photon exchange

Table 1: GMp expected systematic uncertainties on the cross section.

precision of these measurements will greatly benefit other measurements of the proton form factors that rely on the proton cross section, and this measurement will also provide an extraction of G_M^p, which is needed for accurate determination of G_E^p from future polarization transfer measurements.

References

[1] C. Hyde, B. Michel, C. Munoz Camacho, J. Roche *et al.*, Jefferson Lab experiment E12-06-114.

[2] B. Wojtsekhowski, R. Lindgren, and N. Liyanage, Hall A Status Report 2006 (2007) 16.

[3] M. Pegoraro, Proceedings of the Fourth Workshop on Electronics for LHC Experiments, CERN/LHCC/98-36, (1998) 257.

[4] J.-P. Chen and D. Armstrong, Hall A Status Report 2004 (2005) 20.

[5] A. Acha *et al.*, Phys. Rev. Lett. **98** (2007) 032301.

[6] L. Andivahis *et al.*, Phys. Rev. **D50** (1994) 5491.

[7] W. Bartel *et al.*, Nucl. Phys. **B58** (1973) 429.

[8] C. Berger, V. Burkert, G. Knop, B. Langenbeck, and K. Rith, Phys. Lett. **B35** (1971) 87.

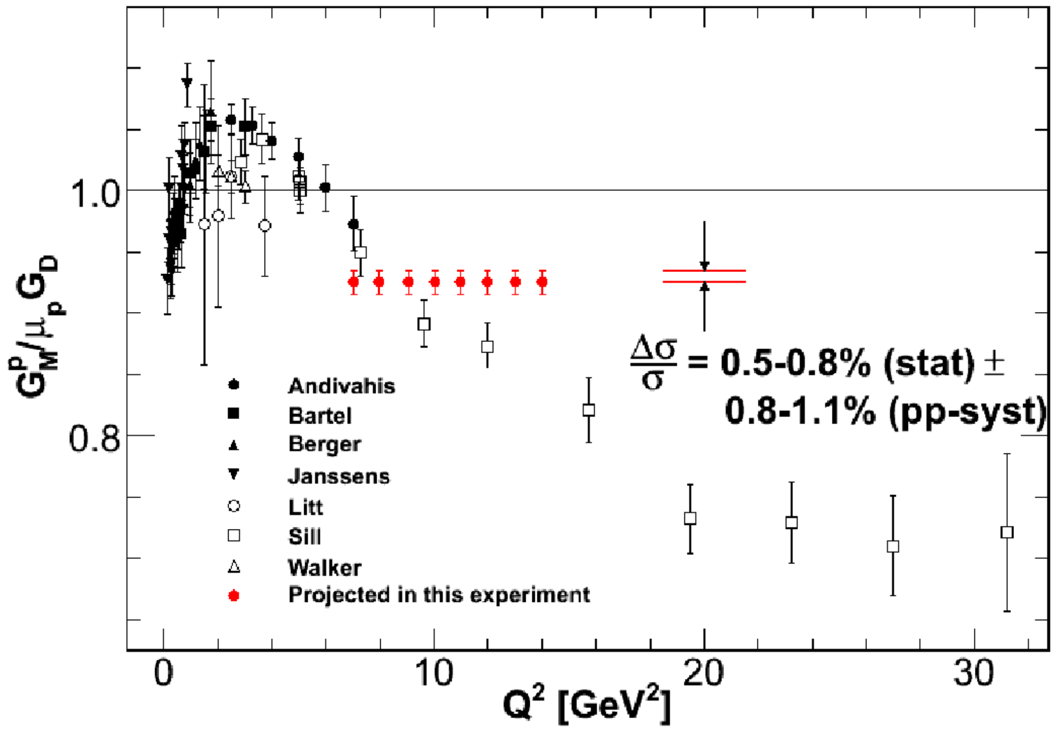

Figure 3: Published world data (Refs. [6, 7, 8, 9, 10, 11, 12]) for $G_M^p/\mu_p G_D$ as a function of Q^2, and the expected results for the proposed measurements. The uncertainties do not include the normalization uncertainty.

[9] T. Janssens, R. Hofstadter, E. B. Hughes, and M. R. Yearian, Phys. Rev. **142** (1966) 922.

[10] J. Litt *et al.*, Phys. Lett. **B31** (1970) 40.

[11] R. C. Walker *et al.*, Phys. Rev. **D49** (1994) 5671.

[12] A. F. Still *et al.*, Phys. Rev. **D48** (1993) 29.